Neural-Network Based Prediction of Inelastic Response Spectra

Sofiane Hammal [a*], Nouredine Bourahla [b], Nasser Laouami [c]

[a] Department of Civil Engineering, University of Blida1, 09000 Blida, Algeria.

[b] Ecole Nationale Polytechnique, Civil Engineering Department, Laboratory LGSDS, Algiers, Algeria.

[c] CGS, National Center of Applied Research in Earthquake Engineering, 01 Rue Kaddour Rahim BP.252, Hussein-Dey, Algiers, Algeria.

Abstract

The prediction of the nonlinear seismic demand for a given hazard level is still a challenging task for seismic risk assessment. This paper presents a Ground Motion Prediction Model (GMPE) for efficient estimation of the inelastic response spectra of 5% damped Single Degree of Freedom (SDOF) systems, with Elastic-Perfectly-Plastic hysteretic behavior in terms of seismological parameters and structural properties. The model was developed using an Artificial Neural Network (ANN) with Back-Propagation (BP) learning algorithm, by means of 200 records collected from KiK-Net database. The proposed model outputs an inelastic response spectra expressed by a 21 values of displacement amplitudes for an input set composed of three earthquake parameters; moment magnitude, depth and source-to-site distance; one site parameter, the shear wave velocity; and one structural parameter, the strength-reduction factor. The performance of the neural network model shows a good agreement between the predicted and computed values of the inelastic response spectra. As revealed by a sensitivity analysis, the seismological parameters have almost the same influence on the inelastic response spectra, only the depth which shows a reduced impact. The advantage of the proposed model is that it does not require an auxiliary elastic GMPE, which makes it easy to be implemented in Probabilistic Seismic Hazard Analysis (PSHA) methodology to generate probabilistic hazard for the inelastic response.

Keywords: Inelastic Response Spectra; Ground Motion Prediction Equation; Attenuation Relationship; Artificial Neural Network.

1. Introduction

Predicting the seismic demand for a given hazard level is a critical part in both seismic design and seismic evaluation of existing structures. Several researchers have proposed the peak inelastic displacement (S_{di}) as an adequate option to assess the seismic demand. This led to simplified seismic analysis procedures that are based on the peak inelastic displacement of a Single Degree of Freedom (SDOF) system with a bilinear hysteresis behavior, having a period equal to the fundamental period of the structure, and a lateral strength determined via a pushover analysis [1]. Well-known methods such as the Capacity Spectrum Method (CSM) are based on superimposing the seismic capacity over the corresponding seismic demand for a given hazard level to determine the expected response of the structure. Basically, the capacity curve relies on the use of nonlinear static analysis (pushover method) while the seismic demand is a representation of the earthquake ground motion, generally it is obtained directly by time-history analyses of inelastic SDOF systems, or indirectly from elastic spectra [2].

Expressing the response spectra for a given site in terms of seismological parameters and structural properties has received much interest; a large number of studies have been conducted to develop the Ground Motion Prediction

---

Equation (GMPE), which express the response spectra in terms of seismological parameters in the form of attenuation relationships [3, 4]. Two approaches have been proposed to estimate the inelastic seismic demand. In the first approach, the inelastic response is derived from the elastic one through a reduction coefficients, which has been criticized and many researchers contend that these reduction factors used in seismic code are highly simplified, and have shown that they depend on the natural period, local site condition, Magnitude and source to site distance [5]. To overcome this shortcoming, a second approach was proposed which consist of developing Ground Motion Prediction Equations (GMPEs) of inelastic response spectra, without the need to resort first to elastic spectra.

Most of the ground motion prediction models of inelastic response spectra are based on regression analysis, whereas, the objective of this work is to predict the inelastic response spectrum and analyze the effects of seismological parameters using feed forward artificial neural network (ANN) with a gradient back-propagation rule for the training. For this purpose, a database of inelastic response spectra is constituted using 5% damped SDOF systems subjected to 200 strong ground motion components strategically extracted from the KiK-Net strong-motion network in Japan. To model the hysteresis behavior of the structure, the Bouc-Wen model [6] is employed. Nonlinear dynamic analyses of SDOF systems are performed using the constant strength approach, considering various vibration periods at different strength levels [7, 8]. The inputs to the ANN are the magnitude (M), the focal depth (d), the source-to-site distance (R), the shear wave velocity (V_{s30}) and the reduction factor (q), while the target outputs are the amplitudes of the inelastic response spectra (S_d) for a frequency range. Subsequently, a sensitivity analysis is carried out in an attempt to capture the influence of the seismological parameters on the response spectra.

2. Ground Motion Database

The strong motion database developed in this study includes approximately 200 records from 8 events ranging between M= 5.4 to 7.3 which occurred in Japan during the period 2000 - 2016. The earthquake ground motions were attentively selected from the KiK-Net database, the distributions of the records versus earthquake magnitude and source-to-site distance are presented in Figure 1. A special attention is paid to the selection of samples or data as it may significantly improve the performance of the trained neural network. All the selected ground motion records have a PGA higher than 0.05g.
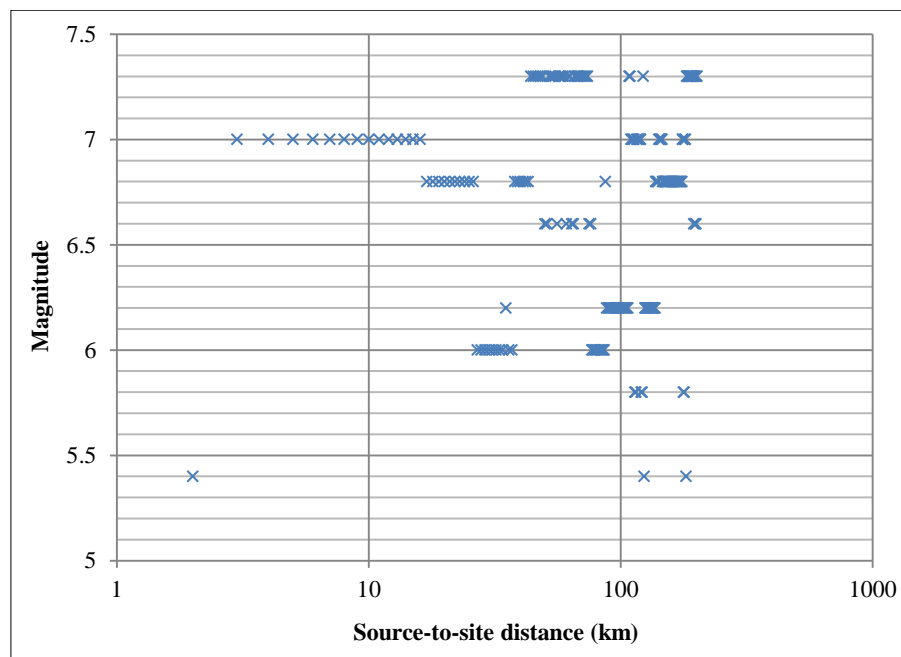

Figure 1. Magnitude versus Source-to-site distance distribution

3. Site condition, Epicentral Distance and Magnitude Distribution

Site condition parameters are used to quantify the influence of local site geology on the characteristics of the ground motion. The KiK-Net database provides geotechnical information on the site of each station. This information consists of the lithology description and the velocity profile for both P and S waves.

Local site effect is one of the most important aspects in earthquake engineering design and is often characterized by a set of simplified parameters, such as site class based on site predominant period [9], site class based on geological and geotechnical description of soil layers and site period [10], and the average soil shear-wave velocity down to a depth of 30 m (V_{s30}) used by many recent ground motion prediction equations (GMPE) [11, 12].

In the present study, the V_{s30} is introduced as a governing parameter to characterize the site effect on the response of structures. The V_{s30} for each site is calculated using the following equations:

$$V_{s30} = \frac{30}{\sum_{i=1}^{n} \frac{h_i}{v_i}}$$ (1)

Where: h_i: thickness of ith layer, v_i: shear wave velocity.

Figure 2 shows the distribution of the site classes according to NEHRP classification [13] which is based on the shear wave velocity V_{s30}. More than 68% of the strong ground motions used in this study were recorded on site class C, about 21% on site class D (V_{s30} between 180 and 760 m/s) and 8% on site class B (V_{s30} greater than 760 m/s).
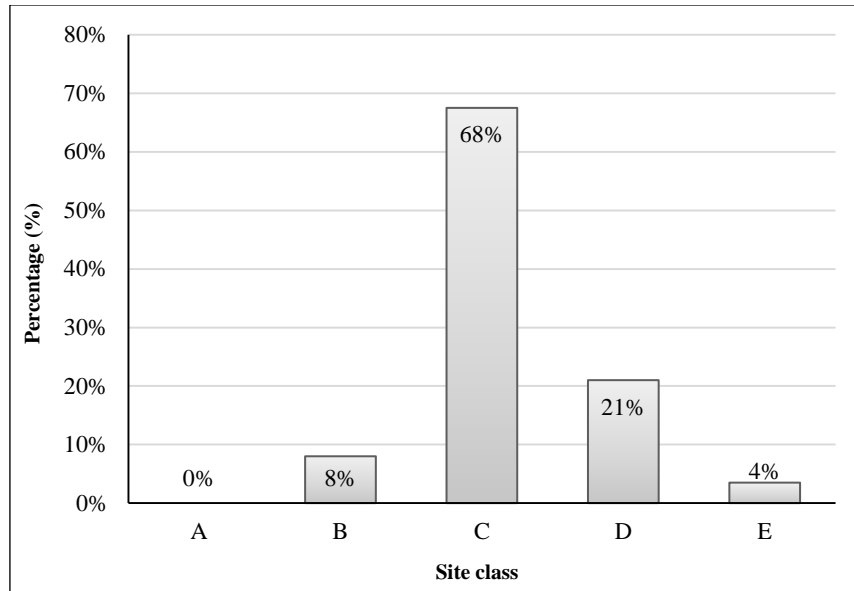

Figure 2. Distribution of ground motion samples according to NEHRP classification of soil sites

4. Computation of Inelastic Response Spectrum

Equivalent Single Degree of Freedom (ESDOF) systems are commonly used in the field of earthquake and structural engineering [14, 15] to approximate the response of Multi Degree of Freedom (MDOF) structures, including regular RC buildings, when the response is dominated by a single mode with a high modal participation factor. Different methods also make use of equivalent SDOF systems to predict damage in structures. [16, 17]

Most of the Ground Motion Prediction Equations for elastic and inelastic response spectra proposed in literature are based on the response of constant-ductility systems and are developed for design purpose [3]. Furthermore, the seismic assessment and design verification are based on the evaluation of the ductility demand of structures with given strength, stiffness and restoring force characteristics. This investigation is predicated on the constant-strength approach. Consequently, five-yield strength reduction factors (q) equal to 1, 2, 3, 4, and 5 are considered.

A set of 21 SDOF systems are considered to cover periods of vibration ranging from 0.1 sec to 4 sec (step 0.2 sec). Yielding strength values (f_y) are computed dividing the elastic strength (F_e), corresponding to the period of interest, by a yield strength reduction factor (q). A total number of 21 000 nonlinear time history analyses were carried out. As illustrated in Figure 2, an Elastic Perfectly Plastic (EPP) model is used.

For an inelastic damped SDOF system subjected to ground acceleration, the differential equation of motion can be expressed as follows:

$$m\ddot{x}(t) + c\,\dot{x}(t) + f(x,x) = \dot{}\ -m\,\ddot{x}_g(t)$$ (2)

Where: m, c and f represent the mass, damping and resisting force of the inelastic system, respectively; $\ddot{x}_g(t)$ denotes the ground acceleration; $\ddot{x}, \dot{x}, x$ represent respectively the acceleration, velocity and deformation of a SDOF.

In this investigation, Bouc-Wen model is selected for its simplicity, stability and it can simulate any extended plastic deformation [6]. Runge-Kutta method is adopted to solve the model differential equation numerically [18]. According to Bouc-Wen, the resisting force $f(t)$ is defined as the sum of the linear part and the hysteretic part, and depends on history of deformation.

$$f(t) = k_p\, x(t) + Q\, z(t)$$ (3)

Where: k_p is the post-yield stiffness; Q is the yield strength (ordinate at origin of creeping part) whereas f_y represents the yielding force; and the adimensional variable $z(t)$ which characterizes the Bouc-Wen hysteresis model:

$$\dot{z}(t) = \frac{\dot{x}(t)}{x_y}\left[A - |z|^\lambda \left(B.sign(\dot{x}z) + \beta\right)\right] \tag{4}$$

Where: $z(t)$ depends on the yield displacement f_y, as well as A, B, λ and β that are the parameters that control the shape of the hysteresis loop. The adopted values are:

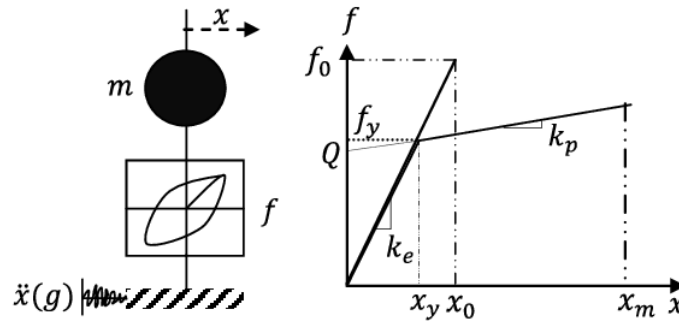$A = 1, B = 0.1, \lambda = 0.9, \beta = 6$ and $k_p = 0$ for bilinear elastic-perfectly plastic system

Figure 3. Elastic-Perfectly-Plastic relationship of inelastic single-degree-of-freedom

5. Artificial Neural Network

Taking into account the particularities of the present study, a Feedforward Multilayer Perceptron FMP is selected. The Feedforward backpropagation (FFBP) is one of the most utilized forward neural networks, it was first described by Rummelhart et al. [19]. The backpropagation technique is a process of iterations that modify the weights from the output layer to input layer until no further correction is required. A simple hidden backpropagation neural network layer can generally approximate any nonlinear function with arbitrary precision [20, 21]. This feature makes FFBP popular for predicting complex nonlinear systems [22, 23] it has been used to develop methods generating spectrum compatible ground acceleration time histories [24] as well as the prediction of ground time history responses [25].

There are several functions such as hyperbolic tangent, sigmoid and linear functions that can be used as activation or transfer function. The type of activation function plays an important role, and allows the introduction of nonlinearity so that it can deal even with complex phenomena. A systematic theory to determine the number of input nodes and hidden layer nodes is unavailable [21]. Therefore, the selection of an architecture of the neural network is determined by trial and error [26, 27]. The concept of the ANN in estimating the inelastic response spectra is illustrated in Figure 4 together with a schematic representation of the input and output parameters.
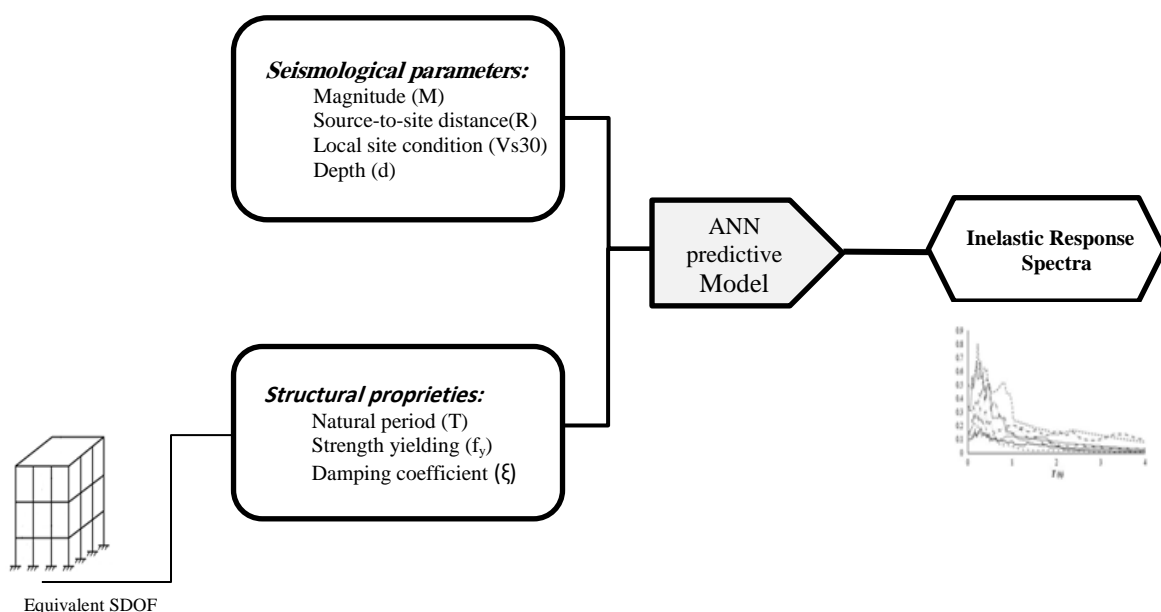

Figure 4. Process of estimating the inelastic response spectra (S$_d$)

Figures 4 and 5 shows the flowchart for the process of computation of the inelastic response spectra. As shown in Figure 5, the constant-strength inelastic response is calculated by reducing the elastic strength of SDOF system from

the corresponding reduction factor. A global flowchart of the procedure used in this study is shown in Figure 5. The selected ground motions from the KiK-Net database are first used to construct the ANN database using the constant-strength approach and then introduced to train, test and validate the ANN model.
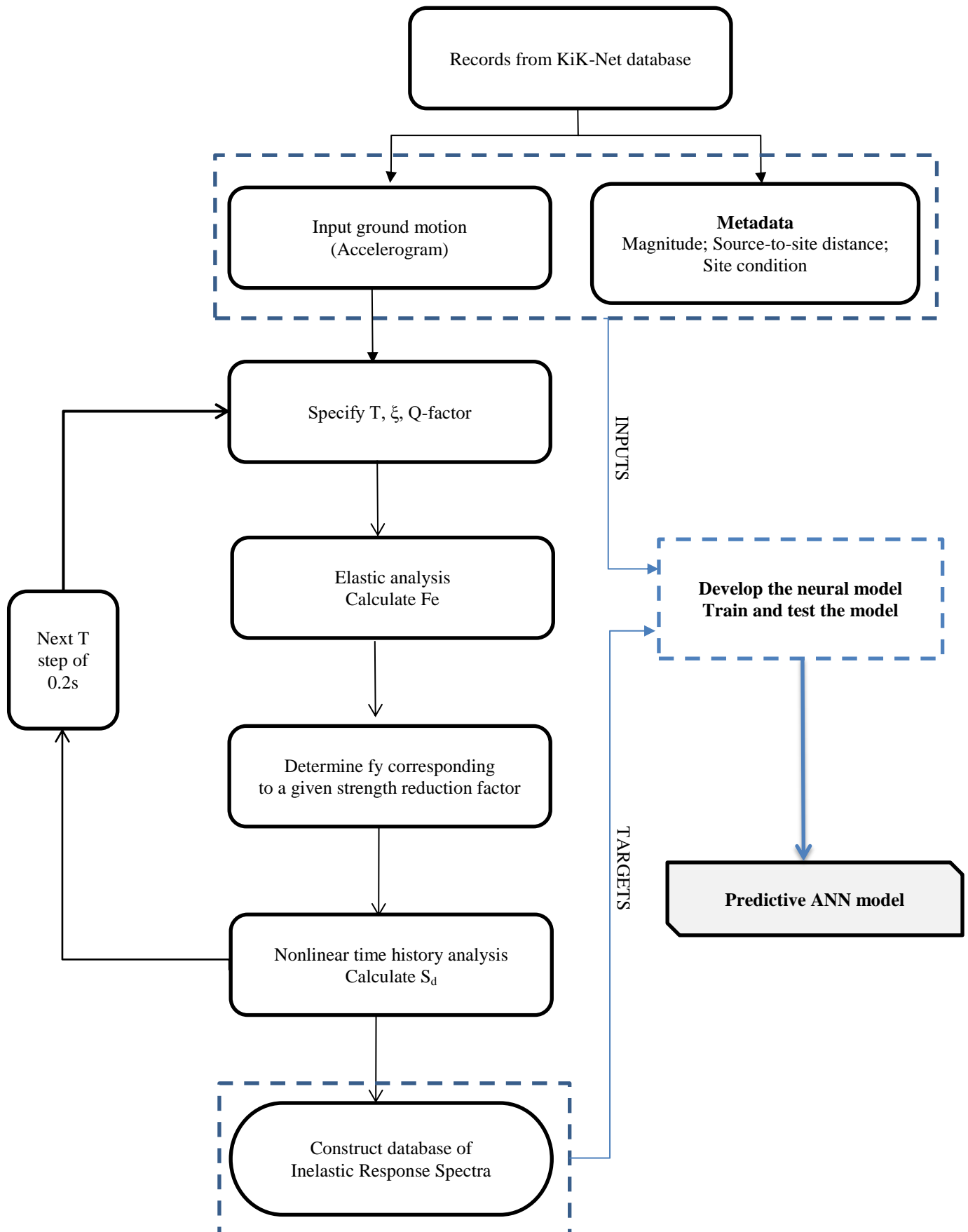

Figure 5. Flowchart presented overall procedure for predicting inelastic response spectra

6. Results and Discussion

6.1. Neural network Topology Optimization

Various neural typologies were tested to define the optimal architecture of a neural model. The results are presented in table 1, which list the Mean Square Error (MSE) and correlation coefficient (R) for different tests using different combinations. Following various tests on the different combination and architecture. It turned out that the inelastic response spectra predicted by the proposed models with five inputs using the combination of tangent hyperbolic function (tanh-sigmoid) as an activation function for the hidden layer and linear function (lin) for the output layer, with ten neurons, appears to be the most accurate (Figure 6).
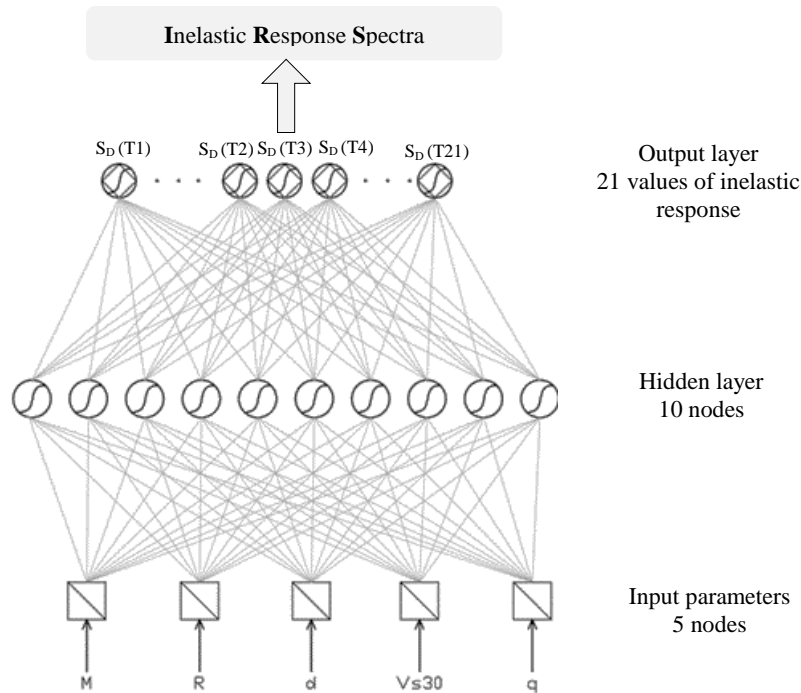
Figure 6. Structure of ANN model

Figure 7 shows the regression curve which plots the values of the inelastic response estimated by the proposed model against the calculated values. The correlation coefficient (R) shows that the values predicted by the neural model are in good agreement with the target values (R=0.93).
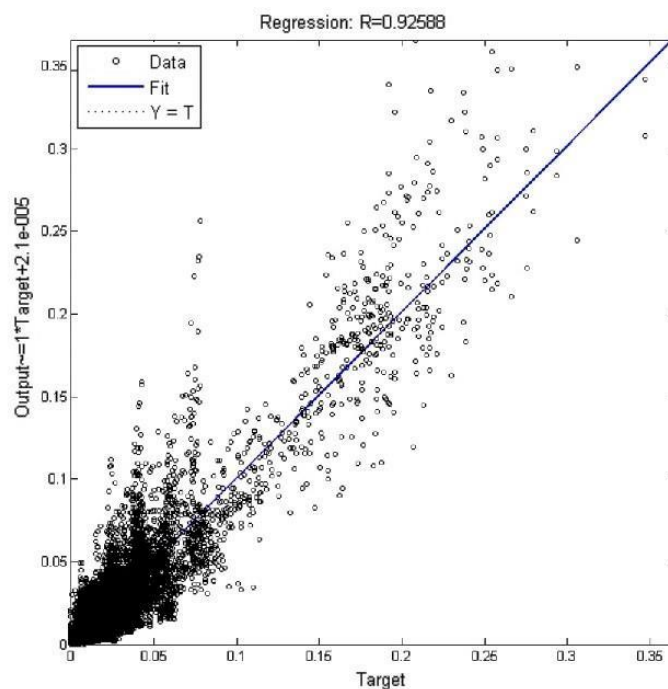
Figure 7. Linear regression between the target and predicted S_d

To evaluate the statistical behavior of the developed model the residuals are plotted against the M, the R and the V_{s30} for predicted inelastic response spectra. As illustrated in Figure 8, generally there is no bias of trend in the residuals. However, It should be noted that in small magnitude events (M=4.5) and in the large distance (R>150 km; Far field) significant bias values were observed with respect to Magnitude and distance. The bias in the model is attributed to insignificant response amplitudes due to the attenuation of the ground motion with Magnitude and Distance.
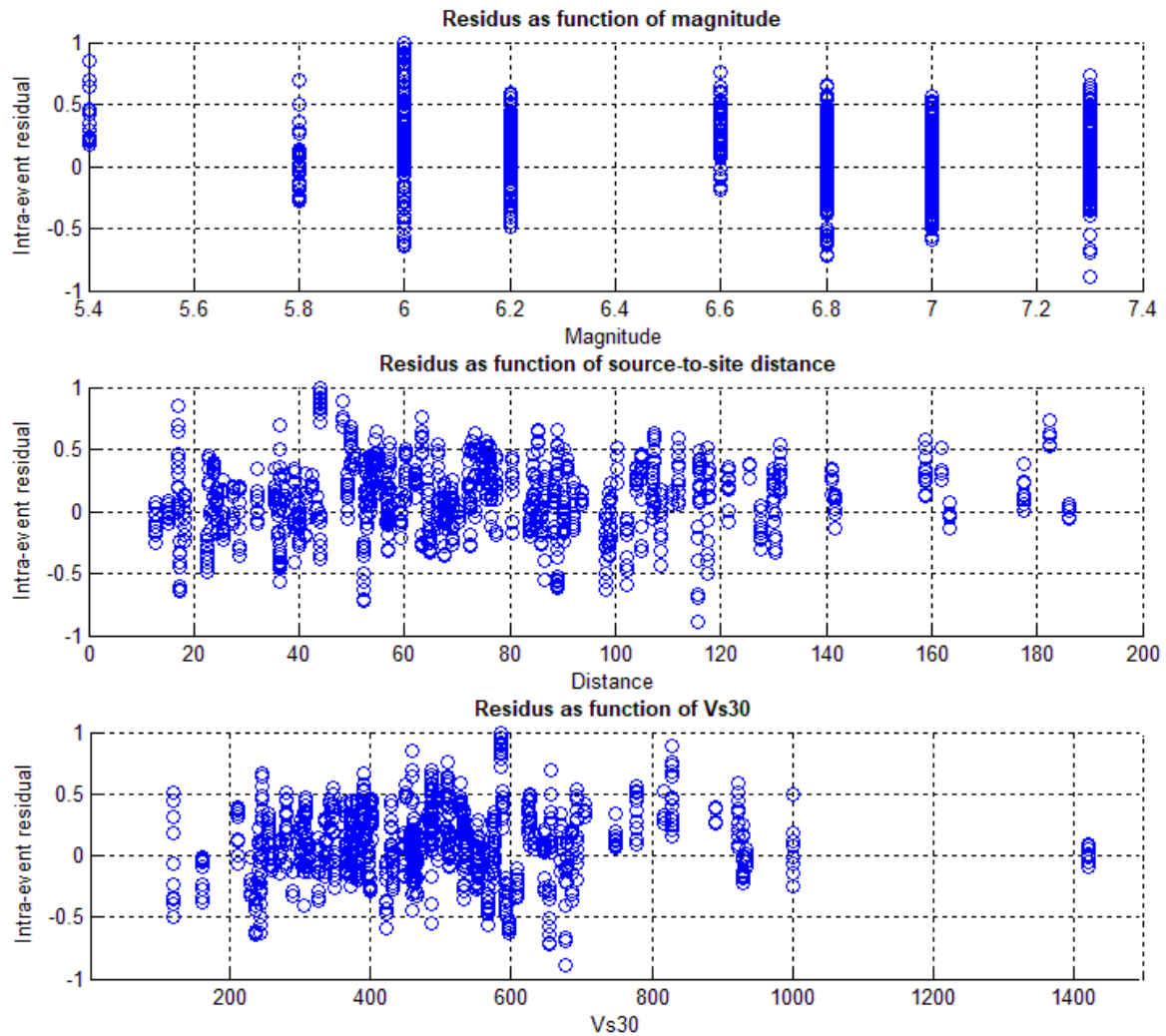

Figure 8. Intra-event residuals as function of distance R, magnitude and V_{s30}

Table 1. Test of different combination of activation function

Activation Function		Performance Criteria				
Layer 01	Layer 02	R_{train}	R_{valid}	R_{test}	R_{all}	MSE
log-sigmoid	log-sigmoid	<0.1	<0.1	<0.1	<0.1	>0.5
log-sigmoid	linear	0.95	0.92	0.91	0.93	0.008
Tanh-sigmoid	linear	0.94	0.92	0.92	0.93	0.007
Tanh-sigmoid	Tanh-sigmoid	0.86	0.83	0.87	086	0.018

6.2. Effect of Intensity Measures on Inelastic Response Spectra

This section presents the effect of the chosen vector-valued seismological parameters on the inelastic response spectra predicted by the ANN model. Figure 9 shows the variation of the S_d amplitudes with natural periods for three values of magnitude (M 5.5, 6, and 6.5) while keeping the same values of: source-to-site distance (R 50 km), Depth (d 10 km) and Shear wave velocity (V_{s30} 180 m/s). The trend of variation for all magnitudes is similar and tends to increase the inelastic displacement demand further in the long-period region (2 s < T < 3.5 s).
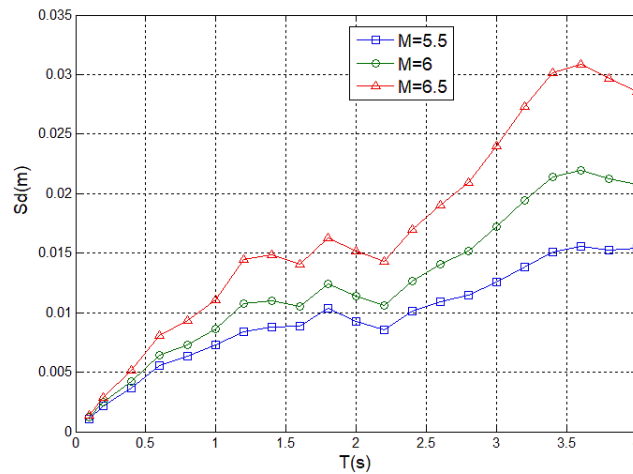
Figure 9. Predicted inelastic response spectra for M in (5.5, 6, and 6.5)

Source-to-site distance-dependent inelastic response spectra are shown in Figure 10 for two scenario: Near field (R 20 km) and Far Field (R 70 km) with the same M, d and V_{s30}. The results indicate clearly that the inelastic deformation demand is still more pronounced in the long-period region with the same trend for both the near and far field scenario. Logical trend is observed, there is systematic increase in the S_d spectra with a decrease in the source-to-site distance.

Figure 10. Predicted inelastic response spectra for R in (20 km, 70 km)

To highlight the influence of the site condition on the inelastic response spectra, the curves corresponding to the spectra predicted by the ANN model are plotted in Figure 11 for three values of V_{s30} (180 m/s, 270 m/s and 360 m/s). It shows that the effect of the V_{s30} is similar to the previous parameters and small values of Vs30 (soft soil) produce larger response than site with high values of V_{s30}.

Figure 11. Predicted inelastic response spectra for V_{s30} in (180 m/s, 270 m/s, 360 m/s)

The reduction factor is used to reduce the yielding strength obtained from a linear analysis in order to take into account the non-linear structural capacities. Figure 12 elucidate further the influence of reduction factor on the inelastic response spectra where each increment of q-factor leads to decreasing nonlinear response. Based on the results illustrated in Figures 9 to 12, the relation between the inelastic response spectra and seismological parameters present a similar trend and all the parameters considered as inputs are more effective in the large-period region.
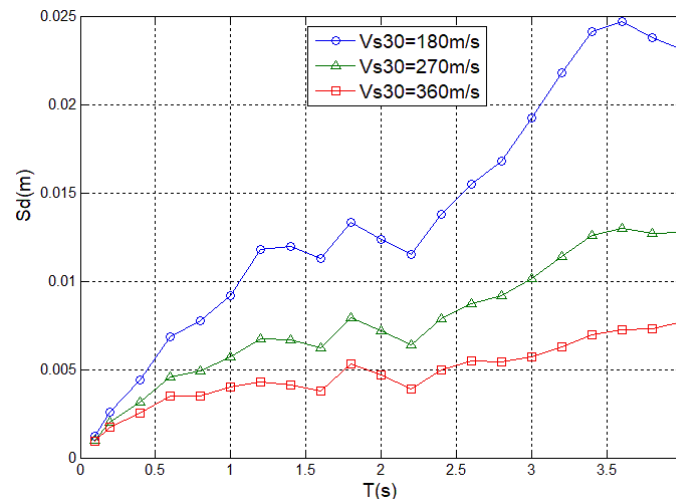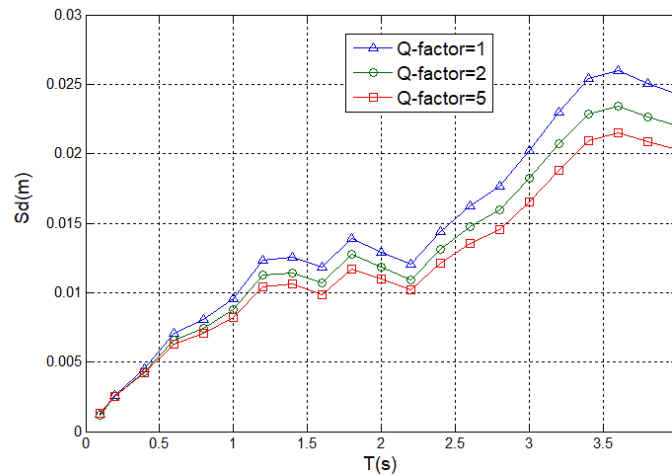

Figure 12. Predicted inelastic response spectra for Q-factor in (1, 2, and 5)

The dependence of the inelastic response spectra on seismological parameters, such as magnitude, distance, and soil condition, was investigated. The obtained results are well substantiated by the physical meaning of the magnitude as an increase in the magnitude values leads to consistent increase of inelastic response demand. It is well known that strong ground motions attenuate with distance, this was clearly reflected in figure 10 where significant reduction in the inelastic response spectra is observed in the far fields. On the other hand, as expected, structures on soft soil foundations are exposed to higher ductility demands than those on stiff soil foundations.

7. Sensitivity Analysis

A sensitivity analysis of the seismological input parameters is performed, in order to gauge the individual influence of each parameter on the S_d spectra. Percentages of synaptic weight P_i that corresponds to each of the four parameters are computed using the following equation [23]:

$$P_i = \frac{\sum_{j=1}^{Nh}\left|w_{ij}^h\right|}{\sum_{i=1}^{N}\sum_{j=1}^{Nh}\left|w_{ij}^h\right|} \tag{5}$$

w_{ij}: synaptic weights of the ANN where $i \in [1..N]$ and $j \in [1..N_h]$, with $N=10$ and $N_h=4$.

The overall results are summarized in Figure 13, which shows that the seismological parameters have almost the same effects on the S_d spectra, whereas the depth has less influence.
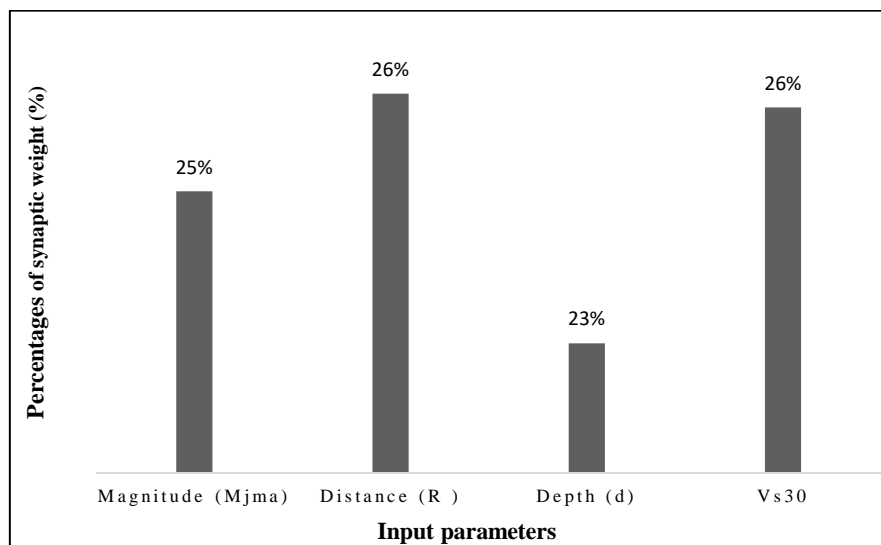

Figure 13. Input sensitivity analysis

8. Conclusion

This work presents a new Ground Motion Prediction Equation (GMPE) for estimating peak inelastic displacement demands of SDOF systems with Elastic Perfectly Plastic (EPP) hysteretic behavior as a function of seismological parameters and structural proprieties. The viscous damping ratio is fixed to 5%. The proposed model has five input parameters consisting of earthquake magnitude, source to site distance, depth, and local site condition and reduction factor.

Unlike most of previous studies based on the constant-ductility approach, this investigation adopts the constant-strength approach in the development of GMPE, which is useful for evaluating the seismic performance of the existing structures. Based on performance criteria such as mean square error (MSR) and correlation coefficient (R), the proposed ANN model predicts the inelastic response spectra with an acceptable precision compared to the real spectra. The result of residual analysis corroborate the model reliability with some bias and poor performance in the small magnitude and far field, this weakness can be justified by the insignificant response amplitudes due to the attenuation of the ground motion with Magnitude and Distance. The use of this GMPE is recommended for events with larger magnitude (M > 5.5) in the near fields (R <150 km). A sensitivity analysis concludes that the seismological parameters have almost the same influence on the inelastic response spectra as predicted by the ANN model except the depth parameter which has a reduced impact.

In practice, the ANN model with only one hidden layer and a limited number of neurons is easy to implement on a spreadsheet or a simple computer program using the synaptic matrices and the bias vector which makes of it a useful tool in both deterministic and probabilistic seismic hazard analysis (PSHA).

9. Funding

10. Conflicts of Interest

The authors declare no conflict of interest.

11. References

[1] Tso, W K, and A. S Moghadam. "Pushover Procedure for Seismic Analysis of Buildings." Progress in Structural Engineering and Materials 1, no. 3 (April 1998): 337–344. doi:10.1002/pse.2260010317.

[2] ATC, Seismic. "Evaluation and retrofit of concrete buildings. vol. 1, ATC-40 report." Redwood City (CA): Applied Technology Council (1996).

[3] Bozorgnia, Yousef, Mahmoud M. Hachem, and Kenneth W. Campbell. "Ground Motion Prediction Equation ('Attenuation Relationship') for Inelastic Response Spectra." Earthquake Spectra 26, no. 1 (February 2010): 1–23. doi:10.1193/1.3281182.

[4] Tothong, P., and C. A. Cornell. "An Empirical Ground-Motion Attenuation Relation for Inelastic Spectral Displacement." Bulletin of the Seismological Society of America 96, no. 6 (December 1, 2006): 2146–2164. doi:10.1785/0120060018.

[5] Rupakhety, R., and R. Sigbjörnsson. "Ground-Motion Prediction Equations (GMPEs) for Inelastic Displacement and Ductility Demands of Constant-Strength SDOF Systems." Bulletin of Earthquake Engineering 7, no. 3 (April 25, 2009): 661–679. doi:10.1007/s10518-009-9117-6.

[6] Wen, Yi-Kwei. "Method for random vibration of hysteretic systems." Journal of the engineering mechanics division 102, no. 2 (1976): 249-263.

[7] Chopra, A. K. "Dynamics of Structures: Theory and Applications to Earthquake Engineering." Prentice Hall, New York, (2001).

[8] Ruiz-García, Jorge, and Eduardo Miranda. "Inelastic Displacement Ratios for Evaluation of Existing Structures." Earthquake Engineering & Structural Dynamics 32, no. 8 (April 28, 2003): 1237–1258. doi:10.1002/eqe.271.

[9] Zhao, J. X. "Attenuation Relations of Strong Ground Motion in Japan Using Site Classification Based on Predominant Period." Bulletin of the Seismological Society of America 96, no. 3 (June 1, 2006): 898–913. doi:10.1785/0120050122.

[10] McVerry, Graeme H., John X. Zhao, Norman A. Abrahamson, and Paul G. Somerville. "New Zealand Acceleration Response Spectrum Attenuation Relations for Crustal and Subduction Zone Earthquakes." Bulletin of the New Zealand Society for Earthquake Engineering 39, no. 1 (March 31, 2006): 1–58. doi:10.5459/bnzsee.39.1.1-58.

[11] Boore, D.M., W.B. Joyner, and T.E. Fumal. "Estimation of Response Spectra and Peak Accelerations from Western North American Earthquakes; an Interim Report, Part 2." Open-File Report (1994). doi:10.3133/ofr94127.

[12] Abrahamson, Norman, and Walter Silva. "Summary of the Abrahamson & Silva NGA Ground-Motion Relations." Earthquake Spectra 24, no. 1 (February 2008): 67–97. doi:10.1193/1.2924360.

[13] Council, Building Seismic Safety. "NEHRP recommended provisions for seismic regulations for new buildings and other structures." FEMA 302 (1997): 303.

[14] Riddell, Rafael, Jaime E. Garcia, and Eugenio Garces. "Inelastic Deformation Response of SDOF Systems Subjected to Earthquakes." Earthquake Engineering & Structural Dynamics 31, no. 3 (2002): 515–538. doi:10.1002/eqe.142.

[15] Mavroeidis, G. P., G. Dong, and A. S. Papageorgiou. "Near-Fault Ground Motions, and the Response of Elastic and Inelastic Single-Degree-of-freedom(SDOF) Systems." Earthquake Engineering & Structural Dynamics 33, no. 9 (June 24, 2004): 1023–1049. doi:10.1002/eqe.391.

[16] Li, Hong Nan, Feng Wang, and Zhao Hui Lu. "Estimation of Hysteretic Energy of MDOF Structures Based on Equivalent SDOF Systems." Key Engineering Materials 340–341 (June 2007): 435–440. doi:10.4028/www.scientific.net/kem.340-341.435.

[17] Prasanth, Tholen, Siddhartha Ghosh, and Kevin R. Collins. "Estimation of Hysteretic Energy Demand Using Concepts of Modal Pushover Analysis." Earthquake Engineering & Structural Dynamics 37, no. 6 (2008): 975–990. doi:10.1002/eqe.802.

[18] Li, Hong-guang, and Guang Meng. "Nonlinear Dynamics of a SDOF Oscillator with Bouc–Wen Hysteresis." Chaos, Solitons & Fractals 34, no. 2 (October 2007): 337–343. doi:10.1016/j.chaos.2006.03.081.

[19] Rummelhart, D.E., McClelland, J.L., and Group, P.R. "Parallel distributed processing: Explorations in the microstructure of cognition." Vol. 1. Foundations. Cambridge, MA: MIT Press (1986).

[20] Aslanargun, Atilla, Mammadagha Mammadov, Berna Yazici, and Senay Yolacan. "Comparison of ARIMA, Neural Networks and Hybrid Models in Time Series: Tourist Arrival Forecasting." Journal of Statistical Computation and Simulation 77, no. 1 (January 2007): 29–53. doi:10.1080/10629360600564874.

[21] Wang, Lin, Yi Zeng, and Tao Chen. "Back Propagation Neural Network with Adaptive Differential Evolution Algorithm for Time Series Forecasting." Expert Systems with Applications 42, no. 2 (February 2015): 855–863. doi:10.1016/j.eswa.2014.08.018.

[22] Günaydın, Kemal, and Ayten Günaydın. "Peak Ground Acceleration Prediction by Artificial Neural Networks for Northwestern Turkey." Mathematical Problems in Engineering 2008 (2008): 1–20. doi:10.1155/2008/919420.

[23] Derras, B., P.-Y. Bard, F. Cotton, and A. Bekkouche. "Adapting the Neural Network Approach to PGA Prediction: An Example Based on the KiK-Net Data." Bulletin of the Seismological Society of America 102, no. 4 (August 1, 2012): 1446–1461. doi:10.1785/0120110088.

[24] Jamshid, G., and Chu-Chieh, J.L. "New method of generating spectrum compatible accelerograms using neural networks". Earthquake Engineering and Structural Dynamics 27, no.4 (1998): 377-396. doi:10.1002/(sici)1096-9845(199804)27:4<377::aid-eqe735>3.0.co;2-2

[25] Derbal, Ismail, Nouredine Bourahla, Ahmed Mebarki, and Ramdane Bahar. "Neural Network-Based Prediction of Ground Time History Responses." European Journal of Environmental and Civil Engineering 24, no. 1 (August 24, 2017): 123–140. doi:10.1080/19648189.2017.1367727.

[26] Hosseinpour, Saeed, and Jafar Najafizadeh. "Seismic Response of Irregular Triangular Alluvial Valleys Under Shear Waves Using Spectral Elements." Civil Engineering Journal 4, no. 11 (November 30, 2018): 2652. doi:10.28991/cej-03091189.

[27] Karsoliya, Saurabh. "Approximating number of hidden layer neurons in multiple hidden layer BPNN architecture." International Journal of Engineering Trends and Technology 3, no. 6 (2012): 714-717.

[28] Sheela, K. Gnana, and S. N. Deepa. "Review on Methods to Fix Number of Hidden Neurons in Neural Networks." Mathematical Problems in Engineering 2013 (2013): 1–11. doi:10.1155/2013/425740.

Appendix I

Synaptic weight matrices and bias vectors for the ANN model.

w1

-0.08273	7.784	6.06	0.93696	-6.2642
1.0767	0.11994	-0.31878	-2.5242	1.4537
0.075649	3.3268	4.7762	-5.396	-4.4799
-0.18466	-1.3965	11.6736	5.5936	7.0363
-0.23223	-7.6644	3.1154	1.5976	-4.143
0.042267	-2.9187	-6.8243	-9.4885	-6.0351
0.18276	-9.8872	-2.7308	-4.0899	0.86523
0.1035	-0.68123	-2.533	1.9296	4.5337
0.07839	-6.5307	-4.9244	-0.73972	6.7169
-0.42446	-1.1956	0.62353	-5.9804	1.7597

w2

-0.69497	1.2582	0.77342	0.0016248	-0.021422	0.00055935	0.0021854	-0.024154	-0.70027	-0.0022681
-0.69733	0.86513	1.2403	0.013469	-0.034106	0.012143	0.0031869	-0.042941	-0.69197	0.36583
-1.1977	0.91281	1.9885	0.023394	-0.043577	0.019466	0.0026424	-0.069414	-1.205	1.2067
-0.65189	0.45265	1.5371	0.0068614	-0.02991	0.0071722	-0.0014466	-0.069488	-0.647	1.2645
-0.7509	0.47741	1.2508	0.022784	-0.03719	0.023451	-0.021925	-0.062693	-0.72151	1.4402
-0.83841	0.26151	1.03	0.027707	-0.037612	0.031124	-0.03018	-0.062018	-0.80181	1.2971
-1.196	0.49005	1.4481	0.046532	-0.064452	0.053732	-0.044039	-0.12464	-1.136	1.5988
-1.0729	0.44047	0.89061	0.040776	-0.05067	0.044849	-0.035713	-0.083898	-1.0314	1.3869
-1.0936	0.26073	0.89589	0.039891	-0.045606	0.041438	-0.038445	-0.065939	-1.0535	1.6196
-1.3234	0.10961	0.97688	0.0541	-0.052664	0.059982	-0.052983	-0.069108	-1.2701	1.3794
-2.1844	0.39598	1.4031	0.083151	-0.076635	0.090104	-0.084084	-0.080215	-2.1072	1.3263
-2.2963	0.42051	1.2458	0.080693	-0.074154	0.084892	-0.086642	-0.067814	-2.2203	1.2239
-2.3437	0.31557	1.4189	0.094641	-0.088948	0.10172	-0.094376	-0.085297	-2.2537	1.3538
-2.4175	0.29894	1.3752	0.10258	-0.096166	0.10959	-0.097868	-0.10066	-2.321	1.2246
-2.2956	0.2035	1.0627	0.09809	-0.090498	0.10089	-0.087067	-0.098918	-2.2064	1.0843
-1.9691	0.25242	0.91327	0.091751	-0.090386	0.093216	-0.071693	-0.11333	-1.8898	1.0263
-1.8086	0.36762	0.8936	0.098733	-0.1023	0.10258	-0.070494	-0.14054	-1.7232	1.0054
-1.6493	0.57106	0.96845	0.10515	-0.10868	0.11292	-0.076605	-0.16067	-1.5543	0.9258
-1.3447	0.59052	0.8688	0.091351	-0.096803	0.098173	-0.06524	-0.14393	-1.2605	0.86493
-1.5417	0.72015	0.87311	0.10132	-0.10887	0.10759	-0.071355	-0.14891	-1.4501	0.97755
-1.5049	0.5505	0.82062	0.096973	-0.10752	0.10309	-0.070286	-0.13399	-1.4173	1.0786

b1	b2
-11.53	-11.53
-4.2793	-4.2793
-14.0707	-14.0707
0.27949	0.27949
3.3898	3.3898
-3.8287	-3.8287
6.1461	6.1461
4.8577	4.8577
10.0282	10.0282
-7.856	-7.856